Characterization of the mangiferin–human serum albumin complex by spectroscopic and molecular modeling approaches

Yuanyuan Yue, Xingguo Chen*, Jin Qin, Xiaojun Yao

Department of Chemistry, Lanzhou University, Lanzhou 730000, PR China

ARTICLE INFO

ABSTRACT

The interactions between mangiferin and human serum albumin (HSA) were investigated by spectroscopy and molecular modeling. The results proved the formation of complex between mangiferin and HSA. Hydrophobic interaction dominated in the association reaction. Mangiferin statically quenched the fluorescence of HSA in a concentration dependent manner positively deviating from the linear Scatchard equation. The binding of mangiferin to HSA lead to changes in the conformation of HSA according to synchronous fluorescence spectra, FT-IR, UV–vis and CD data. The presence of amino acids and metal ion affected the binding constant of mangiferin–HSA complex. Computational mapping of the possible binding sites of mangiferin revealed the molecule to be bound in the large hydrophobic cavity of subdomain IIA.

© 2008 Elsevier B.V. All rights reserved.

1. Introduction

Mangiferin (Fig. 1), a xanthone glucoside, occurs widely in the bark of *Mangifera indica* (Family: Anacardiaceae, Genus: Mangifera) [1]. Mangiferin is recommended in the Indian systems of medicine [2] for the treatment of immunodeficiency diseases such as arthritis, hepatitis, cardiac, mental disorders, cancer, autoimmune disorders, arteriosclerosis and coronary heart disease [3]. Some reports have showed that mangiferin possesses antioxidant [4], antitumor [5], antiviral [6] and immunomodulatory activities [7]. Furthermore, mangiferin has recently been shown to have antidiabetic activity in KK/Ay mice, a genetic model of non-insulin-dependent diabetes mellitus (NIDDM) with hyperinsulinemia [8,9]. Understanding the interaction between mangiferin and protein is of major pharmaceutical and clinical importance. Investigating the interaction of mangiferin to protein can also elucidate the properties of drug-protein complex.

Human serum albumin (HSA) is found to be major protein components of blood plasma [10]. HSA constitutes over half of the total plasma proteins, a concentration of 35–50 g/L, in a healthy individual [11]. It is a globular protein consisting of a single peptide chain of 585 amino acids and is considered to have three specific binding sites (I–III) for high affinity binding of drugs. Each of the sites consists of two subdomains (A and B), and is stabilized by 17 disulfide bridges. The primary pharmacokinetics function of HSA is participating in absorption, distribution, metabolism and excretion of drugs. Therefore, it is often used as a probe to investigate the binding properties of drugs with HSA. It has been shown that the distribution, free concentration and the metabolism of various drugs can be significantly altered as a result of their binding to HSA [12]. Therefore, investigating the interaction of drugs and serum albumins was significant for knowing the transport and distribution of drugs in body, and for clarifying the action mechanism and pharmaceutical dynamics. Yet, no work has been published for the mechanism of the interactions and detailed physicochemical characterizations of mangiferin binding to HSA.

In this study, the interaction of mangiferin with human serum albumin was investigated by biophysical methods mainly fluorescence, UV–vis, FT-IR and CD studies, serve as aids to better understand the mechanism of the drug binding to HSA. The results have been discussed on the binding parameters, the identification of binding sites, the effect of mangiferin on the conformation of HSA, and the nature of forces involved in the interactions. Furthermore, the binding site of mangiferin to HSA was also discussed using automated molecular docking approach.

2. Materials and methods

2.1. Materials

HSA and mangiferin were purchased from Sigma. HSA was essentially fatty acid free, and its molecular weight was assumed to be 66,500 to calculate the molar concentrations. All HSA solutions were prepared in a pH 7.40 buffer solution, and the HSA stock

* Corresponding author. Tel.: +86 931 8912763; fax: +86 931 8912582.
E-mail address: chenxg@lzu.edu.cn (X. Chen).

solution was kept in the dark at 4 °C. All reagents were of analytical reagent grade. NaCl (1.0 M) solution was used to maintain the ionic strength at 0.1. The buffer (pH 7.40) consisted of Tris (0.2 M) and HCl (0.1 M). The pH was measured by using a pH meter (PHSJ-3F), electrode (T-818-B-6) and standard buffer (HI70007P) for calibration, which were made by the Cany Precision Instruments Co., Ltd. (Shanghai).

Tris (0.2 M)–HCl (0.1 M) buffer solution containing NaCl (0.1 M) was used to keep the pH of the solution at 7.40. Dilutions of the HSA stock solution (3.0×10^{-5} M) in Tris–HCl buffer solution were prepared immediately before use. The stock solution (1.0×10^{-3} M) of mangiferin was prepared in ethanol. The double-distilled water was used throughout the experiments.

2.2. Apparatus and methods

The fluorescence measurements were carried out using RF-5301PC Spectrofluorimeter (Shimadzu, Japan) and 1 cm quartz cell, both excitation and emission bandwidths set on 5 nm. The excitation wavelength was 280 nm, and the emission spectra were recorded between 295 and 550 nm with maximum observed at 341 nm. Meanwhile, synchronous fluorescence spectra of HSA in the absence and presence of increasing amount of mangiferin were measured. An electronic thermoregulating water bath (NTT-2100, EYELA, Japan) was used to control the temperature of the samples.

For titration of HSA with mangiferin the following protocol was used. 3.0 mL solution containing appropriate concentration of HSA was titrated by successive additions of a 1.0×10^{-3} M ethanol stock solution of mangiferin (to give a final concentration of 32.26 μM). Titrations were done manually by using trace syringes, and the fluorescence intensity was measured (excitation at 280 nm and emission at 341 nm). All experiments were measured after 3 min at four different temperatures (289, 296, 303 and 310 K). The temperature was maintained by a circulating water jacket throughout the experiment.

UV–vis spectroscopy was performed on Shimadzu UV-240 spectrophotometer at 298 K in the range 245–450 nm using a quartz cuvette with 1 cm pathlength.

FT-IR measurements were carried out at room temperature on a Nicolet Nexus 670 FT-IR spectrometer (GMI Inc., MN, America) equipped with a Germanium attenuated total reflection (ATR) accessory, a DTGS KBr detector and a KBr beam splitter. All spectra were taken via the attenuated total reflection method with resolution of 4 cm^{-1} and 60 scans. The background (containing all system components except protein) was recorded at the same condition and subtracted from the measured spectra of the sample solution to obtain the FT-IR spectra of the protein. The subtraction criterion was that the original spectrum of protein solution between 2200 and 1800 cm^{-1} was featureless [13] (Fig. 1).

CD spectra were recorded between 190 and 290 nm on an Olis DSM1000CD (Olis, GA, USA) at room temperature in a rectangular quartz cuvette with 1 cm pathlength. All spectra were accumulated in triplicate with a bandwidth of 1.0 nm and a resolution of 0.2 nm at a scan speed of 30 nm/min. Each spectrum represented the average

of five successive scans. Induced CD was determined as the CD of the HSA–mangiferin complex sample after subtraction of CD of the protein alone. The results were taken as molar ellipticity ($[\theta]$) in degree cm^2 dmol^{-1}; the α-helical content of HSA was calculated from the $[\theta]$ value at 208 nm using the equation [14]:

$$\alpha\text{-helix } (\%) = \left\{ \frac{-[\theta]_{208} - 4000}{33,000 - 4000} \right\} \times 100 \tag{1}$$

The crystal structure of HSA in complex with R-warfarin was taken from the Brookhaven Protein Data Bank (entry codes 1h9z) [15]. The potential of the 3D structures of HSA was assigned according to the Amber 4.0 force field with Kollman-all-atom charges. Molecular modeling software Sybyl 6.9 was used to generate the 3D structure of all the molecules [16]. The geometry of the molecule was subsequently optimized to minimal energy using the Tripos force field with Gasteiger-Marsili charges with a gradient of 0.005 kcal/mol. FlexX program was applied to calculate the possible conformation of the ligands that binds to the protein. The conformer with RMS (root-means-square) was used for further analysis. Based on this kind of approach a computational model of the target receptor has been built, partial binding parameters of the mangiferin–HSA system were calculated through SGI FUEL workstations.

3. Result and discussion

3.1. Analysis of fluorescence quenching of HSA by mangiferin

Fluorescence quenching is the decrease of the quantum yield of fluorescence from a fluorophore induced by a variety of molecular interactions with quencher molecule. It has been reported that the binding of small molecules to HSA could induce the conformational change of HSA, because the intramolecular forces involved to maintain the secondary structure could be altered, which results in the conformational change of protein [17]. The conformational changes of HSA were evaluated by the measurement of intrinsic fluorescence intensity of HSA before and after addition of mangiferin in the pH 7.40 Tris–HCl buffer. The effect of mangiferin on HSA fluorescence intensity was shown in Fig. 2. The addition of mangiferin caused a gradual decrease in the fluorescence emission intensity of HSA with a conspicuous change in the emission spectra. The shift of the maximum of emission wavelength from 341 to 325 nm was consistent with the fact that the change in the environment
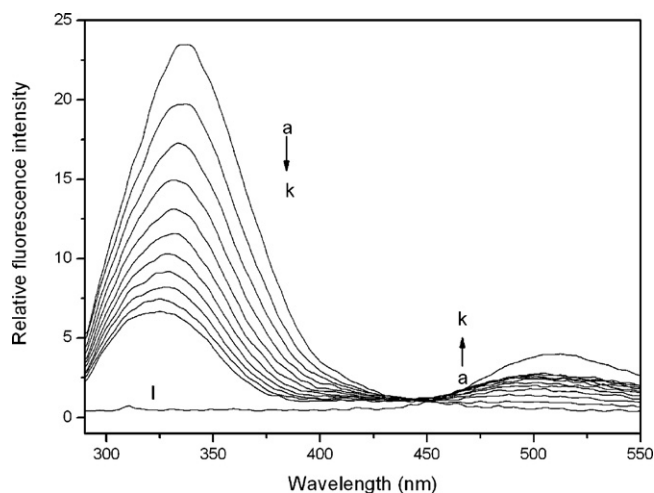

Fig. 1. Molecular structure of mangiferin.

Fig. 2. Effect of mangiferin on fluorescence spectra of HSA (T = 298 K, pH 7.4). (a) 3.0 μM HSA; (b–k) 3.0 μM HSA in the presence of 3.32, 6.62, 9.90, 13.16, 16.39, 19.61, 22.80, 25.97, 29.13 and 32.26 μM mangiferin; (l) 3.32 μM mangiferin.
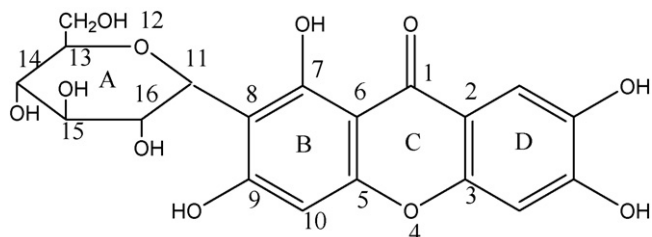
of the tryptophan residues were occurring and an increase of hydrophobicity in the vicinity of this residue takes place. For mangiferin, it caused slight increase in fluorescence emission at 502 nm, which is the characteristic wavelength of bound HSA. This phenomenon might be the result of radiationless energy transfer between mangiferin and HSA [18]. Moreover, the occurrence of isoactinic point at 450 nm might also indicate the existence of bound and free mangiferin in equilibrium [18]. In other words, an isoactinic point was considered as a direct evidence for drug-protein complex formation [19].

3.2. Quenching mechanism, binding constants and number of binding site

The fluorescence quenching processes include static and dynamic quenching. Both mechanisms can be distinguished from each other by the differences in temperature-dependent behavior. It is well known that dynamic quenching process refers to the interaction of quencher and excited state molecule of fluorophore. Since higher temperatures can result in larger diffusion coefficients, the bimolecular quenching constants are expected to increase with increasing temperature. In contrast, a static quenching process refers to the formation of new fluorophore–quencher complex and is often affected by temperature. It will lead to a decrease in the quenching rate constant with raising temperature. According to the above discussions, the static and dynamic can be easily distinguished by the comparison of the values of K at different temperature and absorption spectra of HSA in the presence and absence of quencher. In order to confirm the quenching mechanism, the fluorescence quenching was analyzed according to the Scatchard's equation [20].

$$\frac{r}{D_f} = nK - rK \tag{2}$$

where r is the moles of drug bound per mole of protein, D_f is the molar concentration of free drug, n is binding site multiplicity per class of binding site and K is the association binding constant. Using the fluorescence decrease, the value of K for the complex of mangiferin with HSA was calculated at four different temperatures. A possible quenching mechanism was evident from the Scatchard curves of HSA with mangiferin at different temperatures (289, 296, 303 and 310 K) as shown in Fig. 3. The binding constants and the number of binding sites were summarized in Table 1. The linearity of Scatchard indicates that mangiferin binds to one class of sites on HSA, which was in agreement with the number of binding site n in some degree; and the slopes decreased with increasing temperature, which was consistent with the static type of quenching mechanism.

3.3. Binding mode

Generally, there are essentially four types of non-covalent interactions that could play a key role in ligand binding to proteins. These are hydrogen bonds, van der Waals forces, electrostatic and hydrophobic bonds interactions. The thermodynamic parameters, enthalpy change (ΔH^0) and entropy change (ΔS^0) of binding reaction are the main evidence for confirming binding modes [21]. To obtain such information, the implications of the present results
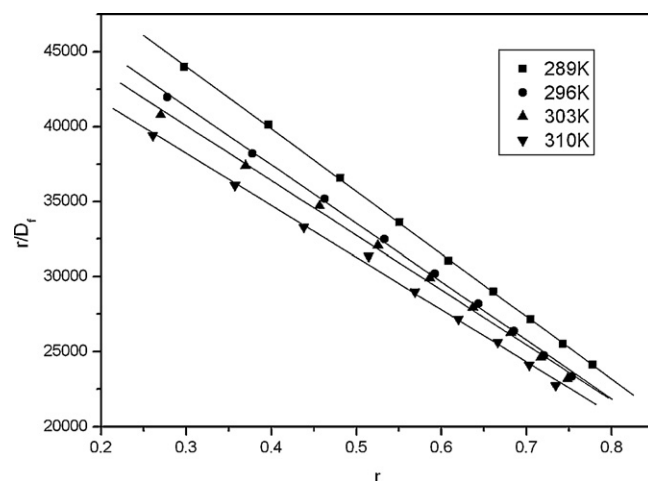

Fig. 3. Scatchard plot for the HSA–mangiferin system at pH 7.4. [HSA] = 3.0 μM; λ_{ex} = 280 nm and λ_{em} = 341 nm.

have been discussed in conjunction with thermodynamic characteristics obtained for mangiferin binding, and the thermodynamic parameters were calculated from the Van't Hoff equation.

$$\ln K_T = \frac{-\Delta H^0}{RT} + \frac{\Delta S^0}{R} \tag{3}$$

K_T is the binding constant at temperature T and R is gas constant. The enthalpy change (ΔH^0) is calculated from the slope of the Van't Hoff relationship. The free energy change (ΔG^0) is estimated from the following relationship:

$$\Delta G^0 = \Delta H^0 - T\Delta S^0 \tag{4}$$

The temperatures chosen were 289, 296, 303 and 310 K at which HSA did not undergo any structural degradation. According to the binding constants at the four temperatures, the thermodynamic parameters were determined from linear Vant'Hoff plot (Fig. 4) and
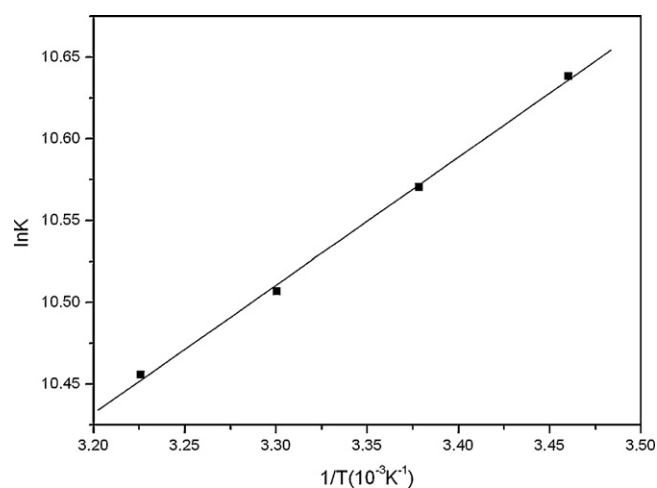

Fig. 4. Van't Hoff plot for the interaction of HSA and mangiferin in Tris–HCl buffer, pH 7.40.

Table 1
Binding parameters and thermodynamic parameters of HSA–mangiferin.

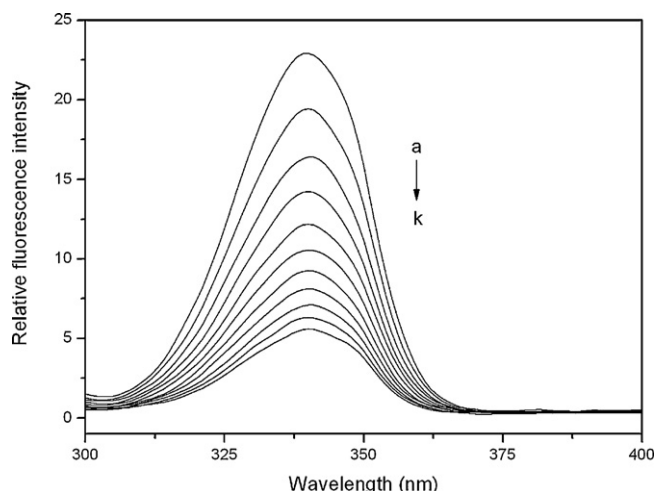| pH	T (K)	K ($\times 10^4$ M^{-1})	n	ΔG^0 (kJ mol^{-1})	ΔS^0 (J mol^{-1} K^{-1})	ΔH^0 (kJ mol^{-1})
7.4	289	4.17	1.35	−25.56	65.87	−6.52
	296	3.90	1.39	−26.02		
	303	3.66	1.36	−26.48		
	310	3.47	1.40	−26.94		

Fig. 5. Synchronous fluorescence spectra of HSA (3.0 μM) in the presence of different concentrations of mangiferin (a–k): [mangiferin] = 0, 3.32, 6.62, 9.90, 13.16, 16.39, 19.61, 22.80, 25.97, 29.13 and 32.26 μM; $\Delta\lambda = 60$ nm.

Fig. 6. Absorbance spectra of HSA and HSA–mangiferin system. Mangiferin concentrations: (a–i) 0, 3.32, 6.62, 9.90, 13.16, 16.39, 19.61, 22.80 and 25.97 μM; [HSA] = 3.0 μM; (j) the spectra of mangiferin, pH 7.40, $T = 298$ K.

were presented in Table 1. Ross and Subramanian [21] have characterized the sign and magnitude of the thermodynamic parameter associated with various individual kinds of interaction that may take place in protein association processes. Accordingly, the negative values of enthalpy (ΔH^0) of the interaction of mangiferin and HSA indicated that the binding was mainly enthalpy-driven and the entropy (ΔS^0) value was unfavorable for it. A positive ΔS^0 value is frequently taken as a typical evidence for hydrophobic interaction from the point of view of water structure. The negative ΔH^0 value (-6.52 kJ mol^{-1}) observed cannot be mainly attributed to electrostatic interactions since for electrostatic interactions ΔH^0 is very small, almost zero [22]. The negative ΔH^0 and positive ΔS^0 values obtained in case of mangiferin therefore indicated that the hydrogen bonding and hydrophobic interactions played a role in the binding of mangiferin to HSA [23].

3.4. Changes of the protein's secondary structure induced by drug binding

Synchronous fluorescence spectroscopy involves simultaneous scanning of the excitation and emission monochromators while maintaining a constant wavelength interval between them. Yuan et al. [24] suggested that a useful method to study the environment of amino acid residues was the measurement of the possible shift in the wavelength of the emission maximum corresponding to the changes of the polarity around the chromophore molecule. When the wavelength interval ($\Delta\lambda$) is fixed at 60 nm, the synchronous fluorescence gives the characteristic information of tryptophan residues [25]. In this work, synchronous fluorescence spectra of HSA with various amounts of mangiferin was recorded at $\Delta\lambda = 60$ nm (Fig. 5) in order to explore any structural changes of the protein molecule on addition of mangiferin. The addition of the drug led to a dramatic decrease in the fluorescence intensity with a slight shift of emission to a shorter wavelength from 341 to 338 nm. It might be referred to a change in the conformation of tryptophan micro-region [26] caused by the interaction of HSA with mangiferin.

UV–vis absorption measurement is a simple method and applicable to explore the structural change [27] and to know the complex formation [28]. The absorption spectra of the HSA of the tryptophan are sensitive to the microenvironment surrounding the chromophore. It can be seen from Fig. 6 that a blue shift of maximum peak position was noticed due to formation of a complex between the drug and HSA [29]. This also indicated that the pep-
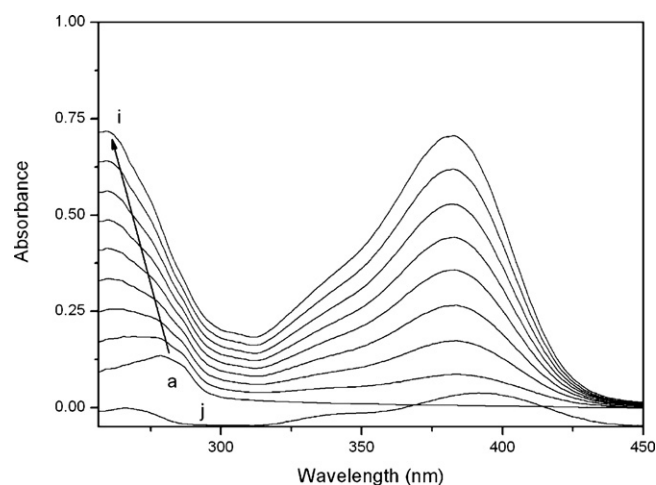
tide strands of protein molecules extended further more upon the addition of mangiferin to HSA [29].

In addition to the fluorescence spectrum, circular dichroism (CD) techniques have proved to be an alternative effective method to measure the conformational transitions of a protein. Fig. 7 shows the CD spectrum of HSA dependent on the mangiferin concentrations. The characteristic peaks at 208 and 222 nm, respectively, are ascribed to the α-helix structure of protein. The reasonable explanation is that the negative peaks between 208 and 209 nm and 222–223 nm are both contributed to $n \rightarrow \pi^*$ transfer for the peptide bond of α-helical [30]. However, the CD spectra of HSA in the presence and absence of mangiferin were similar in shape, indicating that the structure of HSA after addition of mangiferin was also predominantly α-helix. From the above results, it was apparent that the effects of mangiferin on HSA caused a conformational change of the protein, with the loss of helical stability. The calculated results exhibited a reduction of α-helical structures from 55.76 to 52.77 and 50.01% at a molar ratio of HSA to mangiferin in 1:2, 1:4, respectively.

Fig. 8 was the FT-IR spectra of free HSA and its mangiferin complexes in Tris–HCl buffer solution at 298 K. Infrared spectra of proteins exhibit a number of the amide bands, which represent different vibrations of the peptide moiety. Among these amide bands of the protein, the protein amide I in the region
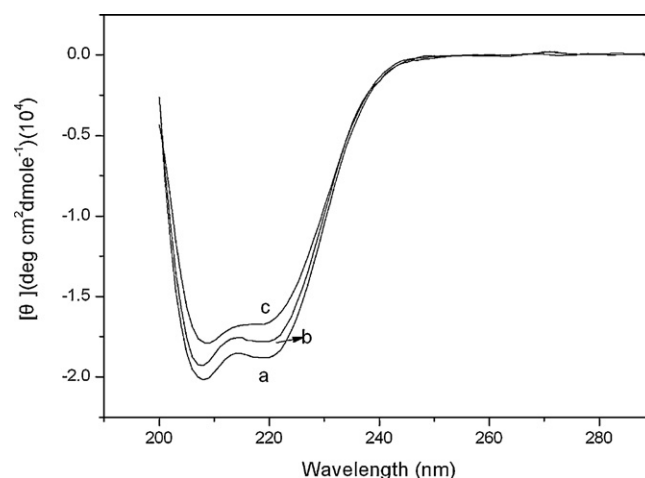

Fig. 7. CD spectra of HSA–mangiferin complexes at pH 7.4; $T = 298$ K. (a) 3.0 μM HSA; (b) 3.0 μM HAS + 6.0 μM mangiferin; (c) 3.0 μM HAS + 12.0 μM mangiferin.
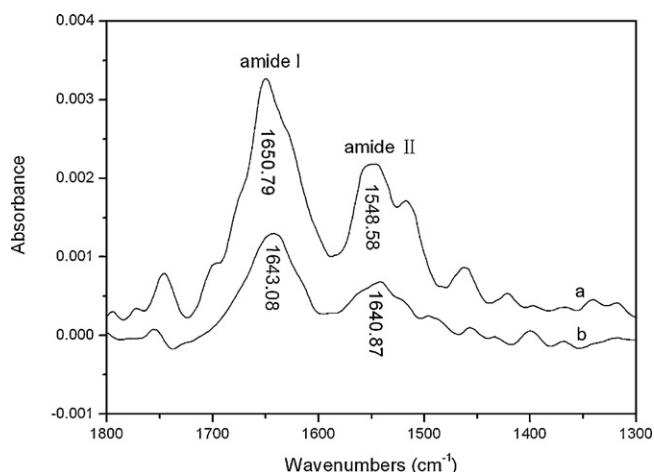
Fig. 8. FT-IR spectra of free HSA (a) and different spectra [(HSA solution + mangiferin solution)–(mangiferin solution)] and (b) in buffer solution in the region of 1800–1300 cm^{-1}. [HSA] = 3.0 × 10^{-5} M, [mangiferin] = 6.0 × 10^{-5} M, pH 7.40 and T = 298 K.
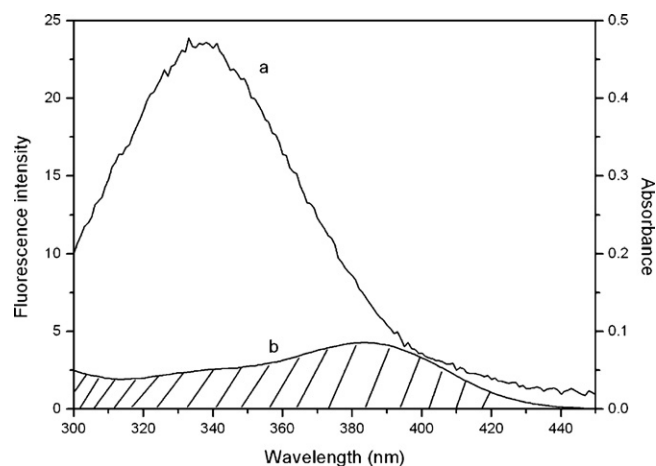

Fig. 9. The overlap of the UV–vis absorption of mangiferin with the fluorescence emission spectrum of HSA: (a) the fluorescence spectrum of HSA and (b) the UV–vis absorbance spectrum of mangiferin. C_{drug}/C_{HSA} = 1:1. pH 7.40 and T = 298 K.

1600–1700 cm^{-1} (mainly C=O stretch) and amide II band in the region 1500–1600 cm^{-1} (C–N stretch couple with N–H bending mode) both have a relationship with the secondary structure of protein, and the amide II band absorbance intensity has been reported to be proportional to the amount of protein absorbed, and is believed not to be very sensitive to the conformation of the protein [31]. Fig. 8 shows the FT-IR spectra and difference spectra of HSA. It could be found that peak positions of amide I band (1650.79 cm^{-1}) and amide II band (1548.58 cm^{-1}) have obvious shift after mangiferin was added, and the intensities of the amide I decreased in the spectra of free HSA. It was important to note that the decrease in the intensity of amide I band was due to the decrease of the proportion of protein α-helix structure [32]. These results indicated that mangiferin interacted with the C=O and C–N groups in the protein polypeptides. The mangiferin–HSA complexes caused the rearrangement of the polypeptide carbonyl hydrogen bonding network and finally the reduction of the protein α-helical structure.

3.5. Energy transfer from HSA to mangiferin

Fluorescence resonance energy transfer (FRET) is a nondestructive spectroscopic method that can monitor the proximity and relative angular orientation of fluorophores, the donor and acceptor fluorophores can be entirely separate or attached to the same macromolecule. It occurs when the emission spectrum of the donor overlaps with the absorption spectrum of the acceptor. The dependence of energy transfer rate on interaction distance has been widely used to measure the distance between donor and acceptor. Generally, the maximum distance is in the range of 7–10 nm [33]. The distance from the tryptophan residue (donor) to the bound drug (acceptor) in HSA can be calculated according to the Förster's theory [34]. The efficiency of energy transfer (E) is related to the distance R between donor and acceptor by

$$E = \frac{1 - F}{F_0} = \frac{R_0^6}{R_0^6 + r^6} \tag{5}$$

where r is the binding distance between donor and receptor, and R_0 is the critical distance when the efficiency of transfer is 50%.

$$R_0^6 = 8.79 \times 10^{-25} k^2 N^{-4} \Phi J \tag{6}$$

In Eq. (6), k^2 is the orientation factor between the emission dipole of the donor and the absorption dipole of the acceptor. N is the refracted index of the medium, Φ is the fluorescence quantum yield

of the donor, and J is the overlap integral of the fluorescence emission spectrum of the donor and the absorption spectrum of the receptor, which could be calculated by the equation:

$$J = \frac{\sum F(\lambda)\varepsilon(\lambda)\lambda^4 \Delta\lambda}{\sum F(\lambda)\Delta\lambda} \tag{7}$$

where $F(\lambda)$ is the corrected fluorescence intensity of the donor in the wavelength range λ to $\lambda + \Delta\lambda$ and $\varepsilon(\lambda)$ is the extinction coefficient of the acceptor at λ. On the basis of these relationships, J, E and R_0 can be calculated; then, the value of r also can be calculated.

The overlap of the absorption spectrum of mangiferin and the fluorescence emission spectra of HSA was shown in Fig. 9. In the present case, $K^2 = 2/3$, $N = 1.336$, $\Phi = 0.118$ [35], according to Eqs. (5)–(7), we could calculate that $R_0 = 1.14$ nm; $E = 0.17$ and $r = 1.92$ nm. The donor-to-acceptor distance (r) is smaller than 7 nm [36], the criteria for energy transfer phenomenon to occur, suggesting that the energy transfer between HSA and mangiferin can occur with high possibility. It also suggested that the binding of mangiferin to HSA was through energy transfer, which was also accord with a static quenching mechanism [37].

3.6. Computational modeling of the mangiferin–HSA complex

The investigation of 3D structure of crystalline albumin showed that HSA contains three homologous domains (I–III): I (residues 1–195), II (196–383), and III (384–585); each domain has two subdomains (A and B). HSA has a limited number of binding sites for endogenous and exogenous ligands that are typically bound reversibly and have binding constants in the range 10^4 to 10^8 M^{-1} [11]. The principal regions of ligand binding sites of albumin are located in hydrophobic cavities in subdomains IIA and IIIA, which are consistent with sites I and II, respectively, and one tryptophan residue of HSA is in subdomain IIA. There is a large hydrophobic cavity present in subdomain IIA that many drugs can bind. To establish which binding site of HSA that mangiferin is located, the complementary applications of molecule modeling have been employed by computer methods to improve the understanding of the interaction of mangiferin and HSA. The Sybyl 6.9 program was chosen to examine the binding mode of mangiferin at the active site of HSA.

The best docking energy result was shown in Fig. 10. It can be seen that mangiferin was situated within subdomain IIA in Sudlow's site I formed by helices. The mangiferin molecular moiety was located within the binding pocket. It was important to note that the tryptophan residue (Trp-214) of HSA was in close proximity
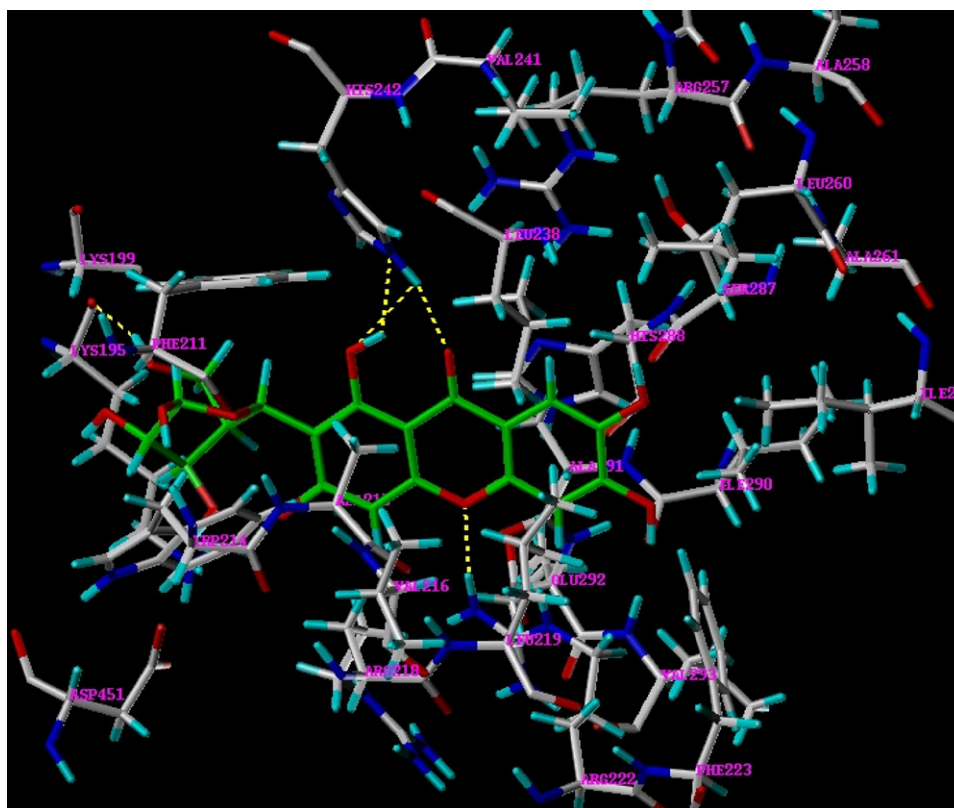
Fig. 10. The binding mode between mangiferin and HSA, only residues around 10 Å of the ligand are displayed. The residues of HSA are represented using gray ball and stick model; and the mangiferin structure is represented by a green one. The hydrogen bond between mangiferin and HSA is represented using yellow dashed line. (For interpretation of the references to color in this figure legend, the reader is referred to the web version of the article.).

to the A- and B-rings of mangiferin suggesting the existence of hydrophobic interaction between them. Furthermore, this finding provided a good structural basis to explain the efficient fluorescence quenching of HSA emission in the presence of mangiferin. The results of molecular modeling suggested that the interaction between mangiferin and HSA was dominated by hydrophobic. However, the interaction between mangiferin and HSA is not exclusively hydrophobic in nature since the several ionic and polar residues in the proximity of the ligand playing important role in stabilizing the drug molecule via hydrogen bond and electrostatic interaction. For instance, His222 is in suitable position to form intermolecular H-bond interaction with 1-O, 7-O. Additionally, Arg222 and Lys195 are able to form intermolecular H-bond with the 4-O and 13-OH. The results suggested that the formation of hydrogen bond decreased the hydrophilicity and increased the hydrophobicity to stability in the mangiferin–HSA system. The calculated binding Gibbs free energy (ΔG^0) is $-14.08 \, kJ \, mol^{-1}$, which is not very close to the experimental data $(-26.02 \, kJ \, mol^{-1})$ to some degree. A possible explanation may be that the X-ray structure of the protein from crystals differs from that of the aqueous system used in this study. All proofs coming from molecular modeling indicated that interaction between mangiferin and HSA is dominated by hydrophobic force; and mangiferin could interact with HSA at site I in subdomain IIA.

3.7. Influences of common metal ions on binding constant

Amino acids are widely distributed in human and metal ions amino acids are vital to human body; and play an essentially structural role in many proteins based coordinate bonds. Therefore, the presence of amino acids and metal ions in plasma may affect interaction of drugs with HSA. We have examined the effects of some

amino acids (L-Leu-OH, L-Proline, L-Lysin, L-Isoleucine, L-Leucine, L-Glu-OH, L-Threonine, L-Hyp-OH, L-Histidine and L-Arginine) and inorganic cations (Zn^{2+}, Ni^{2+}, Fe^{3+}, Al^{3+}, Cu^{2+}, Co^{2+}, Cr^{3+} and Mn^{2+}) on the binding constant of mangiferin–HSA system at 298 K by recording the fluorescence intensity in the range of 300–500 nm upon excitation at 280 nm. The values of binding constant acquired were listed in Table 2. As is shown in Table 2, the presence of Cu^{2+}, Cr^{3+} ions increased the binding constant of mangiferin–HSA complex. The higher binding constant possibly resulted from the formation of metal ion-mangiferin complexes via metal ion bridge [38]. On the contrary, the presence of the tested amino acids and

Table 2
Effects of some common ions and amino acids (6.67 μM) on HSA–mangiferin system.

System	Binding constant (M^{-1})
HSA + mangiferin	$(3.78 \pm 0.022) \times 10^4$
HSA + mangiferin + L-Leu-OH	$(3.66 \pm 0.012) \times 10^4$
HSA + mangiferin + L-Proline	$(3.56 \pm 0.019) \times 10^4$
HSA + mangiferin + L-Lysin	$(3.53 \pm 0.025) \times 10^4$
HSA + mangiferin + L-Isoleucine	$(3.48 \pm 0.011) \times 10^4$
HSA + mangiferin + L-Leucine	$(3.47 \pm 0.035) \times 10^4$
HSA + mangiferin + L-Glu-OH	$(3.23 \pm 0.017) \times 10^4$
HSA + mangiferin + L-Threonine	$(3.28 \pm 0.031) \times 10^4$
HSA + mangiferin + L-Hyp-OH	$(3.51 \pm 0.027) \times 10^4$
HSA + mangiferin + L-Histidine	$(3.42 \pm 0.013) \times 10^4$
HSA + mangiferin + L-Arginine	$(3.20 \pm 0.009) \times 10^4$
HSA + mangiferin + Zn^{2+}	$(3.43 \pm 0.038) \times 10^4$
HSA + mangiferin + Ni^{2+}	$(3.05 \pm 0.043) \times 10^4$
HSA + mangiferin + Fe^{3+}	$(3.27 \pm 0.018) \times 10^4$
HSA + mangiferin + Al^{3+}	$(3.02 \pm 0.040) \times 10^4$
HSA + mangiferin + Cu^{2+}	$(3.93 \pm 0.015) \times 10^4$
HSA + mangiferin + Co^{2+}	$(3.01 \pm 0.036) \times 10^4$
HSA + mangiferin + Cr^{3+}	$(3.96 \pm 0.029) \times 10^4$
HSA + mangiferin + Mn^{2+}	$(3.12 \pm 0.021) \times 10^4$

metal ions decreased the binding constant of mangiferin–HSA complex. Although, mangiferin and metal ion, amino acids for HSA were not located in the same domain, and there was no direct competition between mangiferin and the metal ions, amino acids, the formation of metal ion, amino acids–HSA complexes was likely to effect changes in the conformation of the protein, which may affect mangiferin binding kinetics [39]. This was likely to be caused by a conformational change in the vicinity of the binding site. The disturbance in the binding of drug to HSA can result in pharmacokinetic consequences due to the increase in the free plasma concentration, and these effects are likely to be significant in vivo.

4. Conclusions

The interactions between mangiferin and HSA were investigated by different optical techniques and molecular modeling in this paper. Results showed that mangiferin quenched the fluorescence of HSA through static quenching mechanism. Hydrophobic interactions played a role in the binding process of mangiferin to HSA. The results of these methods were consonant with each other. Additionally, docking calculations found mangiferin to be located in site I of HSA within subdomain IIA. The biological significance of this work was evident since HSA serves as a carrier molecule for multiple drugs and the interaction of mangiferin and HSA was not characterized so far. Hence, the report had a great importance in pharmacology and clinical medicine as well as methodology.

References

[1] R.N. Chopra, S.R. Nayar, I.C. Chopra, Glossary of Indian Medicinal Plants, CSIR, New Delhi, 1956.
[2] S. Ghosal, G. Rao, V. Saravanan, N. Misra, D. Rana, Ind. J. Chem. 35 (1996) 561–566.
[3] J.M. Leiro, E. Alvarez, J.A. Arranz, I.G. Siso, F. Orallo, Biochem. Pharmacol. 65 (2003) 1361–1371.
[4] T. Sato, A. Kawamoto, A. Tamura, Y. Tatsumi, T. Fujii, Chem. Pharm. Bull. 40 (1992) 21–724.
[5] S. Guha, S. Ghosal, U. Chattopadhyay, Chemotherapy 42 (1996) 443–451.
[6] C. Yoosook, N. Bunyapraphatsara, Y. Boonyakiat, C. Kan-tasuk, Phytomedicine 6 (2000) 411–419.
[7] H. Ichiki, T. Miura, M. Kubo, E. Ishihara, Y. Komatsu, K. Tanigawa, M. Okada, Biol. Pharm. Bull. 21 (1998) 1389–1390.
[8] T. Miura, H. Ichiki, N. Iwamoto, M. Kato, M. Kubo, H. Sasaki, M. Okada, T. Ishida, Y. Seino, K. Tanigawa, Biol. Pharm. Bull. 24 (2001) 1009–1011.
[9] T. Miura, N. Iwamoto, M. Kato, H. Ichiki, M. Kubo, Y. Komatsu, T. Ishida, M. Okada, K. Tanigawa, Biol. Pharm. Bull. 24 (2001) 1091–1092.
[10] D.C. Carter, J.X. Ho, Adv. Protein Chem. 45 (1994) 153–203.
[11] T. Peters, All about albumin: biochemistry, genetics and medical applications, Academic Press, San Diego, CA, 1996.
[12] U. Kragh-Hansen, Pharmacol. Rev. 33 (1981) 17–53.
[13] A.C. Dong, P. Huang, W.S. Caughey, Biochemistry 29 (1990) 3303–3308.
[14] Z.X. Lu, T. Cui, Q.L. Shi, Applications of Circular Dichroism and Optical Rotatory Dispersion in Molecular Biology, 1st ed., Science Press, Beijing, 1987.
[15] I. Petitpas, A.A. Bhattacharya, S. Twine, M. East, S. Curry, J. Biol. Chem. 276 (2001) 22804–22809.
[16] G. Morris, SYBYL Software, Version 6.9, Tripos Associates, St. Louis, 2002.
[17] C.Q. Jiang, M.X. Gao, X.Z. Meng, Spectrochim. Acta A 59 (2003) 1605–1610.
[18] W. He, Y. Li, C. Xue, Z. Hu, X. Chen, F. Sheng, Bioorg. Med. Chem. 13 (2005) 1837–1845.
[19] M. Guo, J.W. Zou, P.G. Yi, Z.C. Shang, G.X. Hu, Q.S. Yu, Anal. Sci. 20 (2004) 465–470.
[20] G. Scatchard, Ann. N.Y. Acad. Sci. 51 (1949) 660–673.
[21] P.D. Ross, S. Subramanian, Biochemistry 20 (1981) 3096–3102.
[22] M.H. Rahman, T. Maruyama, T. Okada, K. Yamasaki, M. Otagiri, Biochem. Pharmacol. 46 (1993) 1721–1731.
[23] N. Seedher, B. Singh, P. Singh, Indian J. Pharm. Sci. 51 (1999) 143–148.
[24] T. Yuan, A.M. Weljie, H.J. Vogel, Biochemistry 37 (1998) 3187–3195.
[25] J.N. Miller, Proc. Anal. Div. Chem. Soc. 16 (1979) 203–208.
[26] J.H. Tang, F. Luan, X.G. Chen, Bioorg. Med. Chem. 14 (2006) 3210–3217.
[27] Y.J. Hu, Y. Liu, J. Wang, X. Xiao, S.S. Qu, J. Pharm. Biomed. Anal. 36 (2004) 915–919.
[28] F.L. Cui, J. Fan, J.P. Li, Z.D. Hu, Bioorg. Med. Chem. 12 (2004) 151–157.
[29] K.H. Ulrich, Pharmacol. Rev. 33 (1981) 17–53.
[30] P. Yang, F. Gao, Determination of protein secondary structure by e-transform infrared spectroscopy: a critical assessment. Science Press, 2002.
[31] K.S. Witold, H.M. Henry, C. Dennis, Biochemistry 32 (1993) 389–394.
[32] Y.Y. Yue, Y.H. Zhang, L. Zhou, J. Qin, X.G. Chen, J. Photochem. Photobiol. B 90 (2008) 26–32.
[33] A. Sharma, S.G. Schulman, Introduction to Fluorescence Spectroscopy, John Wiley & Sons, New York, 1999.
[34] L. Stryer, Annu. Rev. Biochem. 47 (1978) 819–846.
[35] L. Cyril, J.K. Earl, W.M. Sperry, Biochemists Handbook, E & FN Epon Led. Press, London, 1961.
[36] B. Valeur, J.C. Brochon, New Trends in Fluorescence Spectroscopy, 6th ed., Springer Press, Berlin, 1999.
[37] Y.Z. Zhang, B. Zhou, Y.X. Liu, C.X. Zhou, X.L. Ding, Y. Liu, J. Fluoresc. 18 (2008) 109–118.
[38] X.F. Liu, Y.M. Xia, Y. Fang, J. Inorg. Biochem. 99 (2005) 1449–1457.
[39] Y.Q. Wang, et al., J. Lumin. 126 (2007) 211–218.